Original Article

HES1 induces *ITPR1*-mediated autophagy to exert anti-metastatic effects in pituitary adenomas

Chunjian Qiu[1#], Yao Yao[2#], Suqin Hu[1], Yixin Xu[3]

[1]Department of Psychiatry, Jinling Hospital, Nanjing University School of Medicine, Nanjing, China; [2]Department of Outpatient, Jinling Hospital, Nanjing University School of Medicine, Nanjing, China; [3]Department of Endocrinology, Jinling Hospital, Nanjing University School of Medicine, Nanjing, China

Contributions: (I) Conception and design: C Qiu, Y Yao; (II) Administrative support: S Hu; (III) Provision of study materials or patients: Y Xu; (IV) Collection and assembly of data: Y Xu, C Qiu; (V) Data analysis and interpretation: Y Yao, S Hu; (VI) Manuscript writing: All authors; (VII) Final approval of manuscript: All authors.

[#]These authors contributed equally to this work.

Correspondence to: Yixin Xu, MD. Department of Endocrinology, Jinling Hospital, Nanjing University School of Medicine, 305 East Zhongshan Road, Nanjing 210002, China. Email: chunjianqiu2023@163.com; Suqin Hu, BD. Department of Psychiatry, Jinling Hospital, Nanjing University School of Medicine, 305 East Zhongshan Road, Nanjing 210002, China. Email: tlingfeng008@163.com.

Background: Pituitary adenomas (PAs) are prevalent intracranial tumors necessitating a comprehensive exploration of their molecular intricacies. This study delved into the molecular interactions among *HES1* (hairy and enhancer of split 1), *ITPR1* (inositol 1,4,5-trisphosphate receptor, type 1), and autophagy to elucidate their contributions to PA progression.

Methods: Our in-depth bioinformatics analysis identified *ITPR1* as a central hub gene in the PA-associated dataset. It exhibited reduced expression in PA and held significant clinical diagnostic relevance. Motivated by this discovery, we investigated the consequences of *ITPR1* overexpression, as well as the use of autophagy inhibitors 3-Methyladenine (3-MA) and Baf A1, while considering the transcriptional influence of *HES1*.

Results: *In vitro* experiments utilizing PA cell lines revealed that *ITPR1* overexpression significantly hindered tumorigenic activities. In contrast, both 3-MA and Baf A1 exacerbated these tumorigenic properties, confirmed by a decreased LC3 II/LC3 I ratio, indicative of autophagy inhibition. Intriguingly, the concurrent introduction of *ITPR1* and these inhibitors mitigated these intensified effects, implying a tumor-suppressive role for *ITPR1*. Further investigations pinpoint *HES1* as a potential upstream regulator of *ITPR1* transcription. Silencing *HES1* lead to reduced *ITPR1* promoter activity, weakening the impact of *ITPR1* overexpression on autophagy. This neutralized the *ITPR1*-mediated suppressions on PA cell activities, including proliferation, invasion, and migration.

Conclusions: In summary, our research uncovered a complex regulatory interplay among *HES1*, *ITPR1*, and autophagy in the context of PA progression. These findings opened up promising avenues for novel therapeutic interventions targeting this intricate network to enhance PA treatment.

Keywords: Pituitary adenomas (PAs); autophagy; inositol 1,4,5-trisphosphate receptor, type 1 (*ITPR1*); hairy and enhancer of split 1 (*HES1*); tumor metastasis

Submitted Jul 26, 2023. Accepted for publication Jan 07, 2024. Published online Feb 28, 2024.
doi: 10.21037/tcr-23-1320
View this article at: https://dx.doi.org/10.21037/tcr-23-1320

Introduction

Pituitary adenomas (PAs), providing for approximately of 15% the majority of intracranial tumors, represent a prevalent and complex pathology (1,2). PA was increasingly recognized in the general population, with an incidence ranging between 3.9 to 7.4 cases annually per 100,000 people. Despite this, their overall prevalence suggests they affect roughly 1 in 1,000 individuals (3). Notably, prolactinomas and nonsecreting PAs make up the majority of these cases. While clinically significant PAs are more common in females, their clinical presentations vary widely. These adenomas can lead to hormone imbalances and visual field defects. In cases with larger tumors, they might also result in hypopituitarism due to the tumor's mass effect (4). Despite associations with various factors such as genetic alterations and environmental influences, the precise etiology of their pathogenesis remains elusive (5,6). Different hormonal types of PA can manifest a variety of symptoms, often due to excessive hormone secretion (2). For instance, prolactinomas can lead to menstrual irregularities and galactorrhea in females, and impotence in males (7). Adenomas that secrete growth hormone can result in acromegaly, marked by enlarged limbs, altered facial features, and skin changes (8). Adenomas secreting corticotropin result in Cushing's disease, marked by central obesity, a moon-like facial appearance, hypertension, and purple striae (9). Current treatments, such as surgical intervention, drug therapy, and radiation therapy, vary in effectiveness based on tumor subtype, size, and aggressiveness (10,11). Despite advances in treatment options, PA remains a significant challenge due to the potential for complications and recurrence in long-term prognosis (12). Early detection is crucial for managing PAs effectively. Prolactinomas are typically treated with dopamine agonists initially, while other PAs often require transsphenoidal surgery as the first-line therapy, reserving medical treatment for cases unresponsive to surgical intervention (13). Consequently, researching effective therapeutic strategies is pivotal to unravel the intricate pathogenesis, deepen our understanding of PA, and enhance patient outcomes.

Autophagy, the intracellular process of lysosomal degradation of cellular components, in a number of physiological and pathological situations, plays a critical regulatory function, including tumorigenesis (14). In cancer, autophagy both impedes tumorigenesis by removing damaged proteins and organelles and supports cancer survival under stress by supplying nutrients (15). The crucial involvement of autophagy in the initiation and progression of tumors has become increasingly emphasized., underscoring the potential for therapeutic strategies that target autophagy (16). Recent study by Lyu *et al.*, highlight the function of autophagy autophagy in the pathogenesis of PA. They demonstrate that tetrandrine (Tet) exhibits anti-PA effects via the MAPK/STAT3 signaling pathway, mediating both autophagy and apoptosis (17). In a study by Kun *et al.*, it was shown that inhibiting hypoxia-inducible factor 1α can counteract temozolomide-induced autophagy in rat PA GH3 cells, thereby boosting the treatment effectiveness of temozolomide against PA (18). However, the complex relationship between autophagy and PA pathogenesis remains incompletely understood. Therefore, it is essential to thoroughly investigate the involvement of autophagy in PA.

Within the realm of PAs, it is becoming evident that certain genes may serve as the linchpin in tumor progression and response to therapies. Among these pivotal genes are *ITPR1* (inositol 1,4,5-trisphosphate receptor, type 1) and *HES1* (hairy and enhancer of split 1). *ITPR1*, an intracellular calcium release channel, is fundamental for a range of physiological processes, including cellular signaling cascades, apoptosis, and cellular proliferation (19). Dysregulation of this gene may interfere with cell differentiation and growth pathways, which may have important implications for tumor behavior. It is worth

Highlight box

Key findings

- Through in-depth bioinformatics analysis, we identified ITPR1 as a central hub gene in a pituitary adenoma (PA)-related dataset. ITPR1 expression is reduced in PAs and has significant clinical diagnostic relevance.

What is known and what is new?

- PAs are prevalent intracranial tumors. Molecular intricacies of PA need comprehensive exploration.
- ITPR1's role as a central hub gene, its clinical diagnostic relevance, and its tumor-suppressive effects in PA.

What is the implication, and what should change now?

- Our findings implied that HES1, ITPR1, and autophagy may be important targets in the treatment of PAs. Relevant actions include the development of new therapeutic approaches focusing on interventions that influence this complex network to improve the outcome of PAs.

mentioning that *ITPR1* acts like an application program in cell signaling, controlling various "applications" within the cell, and the interaction between applications affects the overall cell performance. Dysregulation of *HES1* interferes with cell differentiation and growth pathways, which may have implications for tumor behavior (20). On the other hand, *HES1* is a transcriptional repressor with a renowned function in cellular differentiation and development (21). It is analogous to a regulator that controls gene expression and determines cellular direction. *HES1* determines the direction of cell development, which may have far-reaching consequences in terms of tumor behavior. The potential interplay between *ITPR1* and *HES1*, two hub genes, might hold significant implications for the molecular pathogenesis of PAs and the pursuit of effective therapeutic strategies. We found that *HES1* regulates the expression of *ITPR1*, which affects cell signaling cascades, apoptosis and proliferation. This interaction may play a key role in the molecular pathogenesis of PAs. Given this backdrop, our study's exploration into the interrelation between *HES1*, *ITPR1*, and autophagy not only paves the way for a deeper understanding of PAs but also brings into focus the broader role of hub genes in shaping tumor dynamics.

Considering the clinical challenges of PA and the presence of non-responsive cases, the identification of novel molecular targets is important for proper PA management. The purpose of this research is to elucidate the role of *HES1* and its interactions with *ITPR1* and autophagy in PA cell behavior. In this endeavor, we seek to decipher the intricate regulatory network underlying PA progression, setting the stage for innovative therapeutic approaches for PA patients resistant to current treatments. We present this article in accordance with the MDAR reporting checklist (available at https://tcr.amegroups.com/article/view/10.21037/tcr-23-1320/rc).

Methods

Retrieval of microarray data and analysis of differential expressed genes (DEGs)

For our investigation into PA, two pertinent microarray datasets were sourced from the gene expression omnibus (GEO; https://www.ncbi.nlm.nih.gov/geo/) database: GSE36314, with four prolactinoma and three normal pituitary samples, and GSE119063, encompassing five prolactinoma and four normal pituitary samples. Differential gene expression analysis was carried out on both datasets utilizing the "limma" package in R software. We recognized upregulated DEGs with a fold change (FC) >1.5 and downregulated DEGs with an FC <0.67, all meeting importance threshold of P value <0.05. For a holistic view of the gene expression landscape, DEGs were visualized using the "ggplot2" package in R. The study was conducted in accordance with the Declaration of Helsinki (as revised in 2013).

Screening and analysis of overlapping DEGs

The overlapping up-regulated and down-regulated DEGs in the GSE36314 and GSE119063 datasets were identified using the "VennDiagram" package in R software. The overlapping DEGs were then analyzed for biological process (BP) and Kyoto Encyclopedia of Genes and Genomes (KEGG) pathway enrichment using the Database for Annotation, Visualization and Integrated Discovery (DAVID) database (https://david.ncifcrf.gov/tools.jsp). Results with a P value <0.05 were thought to be statistically significant. The overlapping DEGs were subjected to further scrutiny via the construction of a protein-protein interaction (PPI) network using Cytoscape software. Utilizing the Cytohubba plugin, the top 20 genes were identified based on the BottleNeck, Closeness, and EcCentricity algorithms, which were then used to visualize the PPI network corresponding to the selected genes.

Expression and clinical diagnosis analysis of seven overlapping genes in PPI network

In the PPI network of BottleNeck, Closeness and EcCentricity algorithms, seven overlapping genes were identified, namely *SELL*, *ATF3*, *ITPR1*, *POMC*, *FASN*, *FOXO1* and *CXCR4*. Subsequent examination of these seven gene expressions was conducted within the GSE36314 and GSE19063 data samples. Following this, receiver operating characteristic (ROC) curves for seven genes in the GSE36314 and GSE119063 datasets were generated using the "timeROC" package in R. The area under the curve (AUC) was calculated to assess the clinical diagnostic potential of these genes in the context of PA. This analysis ultimately facilitated the selection of the central hub genes for this study.

Cell culture and treatment

The human PA cell lines HP75 and GH3 were

obtained from Beijing Zhongyuan Ltd., China. Cells were subsequently subcultured in accordance with the manufacturer's directions (22). After transfection with the *ITPR1* plasmid or control vector, cells were treated with autophagy inhibitors: 3-MA (5 mM) or Baf A1 (100 nM) for 24 hours, based on the aforementioned, in conformity with the manufacturer's guidelines.

Cell transfection

Cell transfection was executed utilizing Lipofectamine 2000 as the transfection agent. Cells were cultured in suitable plates and allowed to reach 70–80% confluency prior to transfection. Subsequently, a transfection mixture, composed of the *ITPR1* overexpression plasmid and the transfection agent, was prepared and added to the cells, followed by an incubation period. Simultaneously, to achieve the knockdown of *HES1*, PA cells were subjected to transfection with specific small interfering RNAs (siRNAs) targeting *HES1*, referred to as si-*HES1*-1 and si-*HES1*-2. These transfections were performed when cells attained a confluency of 50–60%, following which the siRNA transfection mix was added to the cells and permitted to incubate for a designated period.

Western blotting (WB) assay

Cellular proteins were extracted by lysing the cells in RIPA buffer, supplemented with protease and phosphatase inhibitors. ABCA protein assay kit was employed to measure the amount of protein in the lysate. By sodium dodecyl sulfate-polyacrylamide gel electrophoresis (SDS-PAGE), equal quantities of protein were loaded, separated, and then deposited onto polyvinylidene difluoride (PVDF) membranes. After that, the membranes were blocked with 5% skim milk at room temperature for an hour. They were then using primary antibodies as a probe specific to the target proteins: ITPR1 (CST, Danvers, USA, 1:1,000), Beclin1 (Abcam, Cambridge, USA, 1:1,000), LC3-I (Sigma-Aldrich, St. Louis, USA, 1:1,000), LC3-II (Novus Biologicals, Centennial, USA, 1:1,000), HES1 (CST, 1:1,000), and β-actin (Sigma-Aldrich, 1:2,000) overnight at 4 ℃. After washing, protein bands were visualized using enhanced chemiluminescence (ECL) detection method after incubation with appropriate secondary antibodies (1:5,000) for 1 hour at room temperature. The intensity was measured using ImageJ software.

Cell proliferation assay

Post-transfection, cells were allocated into 96-well plates and incubated under the stipulated conditions. Proliferation rates were examined at the designated time intervals (24, 48, 72, 96 hours) using the cell counting kit-8 (CCK-8) assay. The CCK-8 reagent was introduced into each well, initiating an additional incubation period that facilitates the reaction between the reagent and viable cells. Following this, the optical density (OD) was determined using a microplate reader set to 450 nm.

Quantitative real-time polymerase chain reaction (qRT-PCR)

Total cellular RNA was isolated using the RNeasy Mini Kit (Qiagen, Hilden, Germany) as per the manufacturer's instructions. First-strand cDNA was synthesized from 1 μg of total RNA employing the PrimeScript RT reagent Kit (Takara, Kusatsu, Japan). Subsequently, qRT-PCR was performed using the TB Green Premix Ex Taq (Takara) on a LightCycler 480 Instrument II (Roche, Basel, Switzerland). The primer sequences utilized in this study were as stated below: *HES1* forward: (5'-TCAACACGACACCGGATAAA-3'), reverse: (5'-TCAGCTGGCTCAGACTTTCA-3'); *ITPR1* forward: (5'-TGCTGTGATTTTAGTGGCGT-3'), reverse: (5'-TCTCCACCCTACCCTTACCT-3'); β-actin forward: (5'-GTCAGTGGTGGACCTGACCT-3'), reverse: (5'-AGGGGAGATTCAGTGTGGTG-3'). Expression levels of *HES1* and *ITPR1* were standardized to the internal reference gene GAPDH. The relative gene expression was determined using the $2^{-\Delta\Delta CT}$ method.

Transwell assay

In the invasion assay, the upper chamber of Transwell inserts was covered with Matrigel. Cells (1×10^5) in serum-free medium were added to the upper chamber, while the lower chamber was filled with media containing 10% fetal bovine serum (FBS) as a chemoattractant. Following a 24-hour incubation, cells that invaded through the Matrigel and reached the underside of the membrane were immobilized using 4% paraformaldehyde and stained cells with DAPI (4',6-diamidino-2-phenylindole) (1:1,000 dilution) for 10 minutes in the dark. Rinse excess DAPI with phosphate-buffered saline (PBS). Observe and quantify the infiltrated cells using a fluorescence microscope. The migration assay

was conducted similarly, but without the Matrigel coating.

Dual-luciferase assay

Cells were plated in 24-well dishes and co-transfected with the suitable luciferase reporter. and Renilla control vectors using Lipofectamine 2000. Post 48 h incubation, cell lysis was performed, and luciferase levels was quantified employing the Dual-Luciferase Assay System (Promega, USA). To adjust for transfection efficiency, firefly luciferase activity was normalized to Renilla luciferase activity. Three independent experiments were performed, and the data were presented as fold induction compared to controls.

Statistical analysis

All experimental results were displayed as mean ± standard deviation (SD) from a minimum of three separate experiments. The Student's *t*-test was used to compare two groups. Comparisons between multiple groups utilized one-way analysis of variance (ANOVA) followed by Tukey's post-hoc analysis. A P value <0.05 was considered statistically significant. All statistical analyses were conducted using the SPSS 25.0 software package (IBM, Armonk, NY, USA). Graphs were generated using GraphPad Prism 8.0 (GraphPad Software, San Diego, CA, USA).

Results

Comparative analysis of DEGs in PA

Analysis of the GSE36314 dataset revealed 71 upregulated and 323 downregulated DEGs (*Figure 1A*). Similarly, the GSE119063 dataset presented 506 upregulated and 3,140 downregulated DEGs (*Figure 1B*). When comparing both datasets, we identified 18 overlapping upregulated and 140 overlapping downregulated DEGs, yielding a total of 158 overlapping DEGs (*Figure 1C*).

Enrichment analysis of 158 overlapping genes

Enrichment analysis of these DEGs revealed associations with several BP terms. Notably, the top BPs included regulation of cell migration, positive regulation of glial cell differentiation, and carnitine biosynthetic process (*Figure 1D*). Furthermore, analysis using KEGG pathways showed notable enrichment in diverse pathways, including apoptosis, cellular senescence, fatty acid degradation, extracellular matrix (ECM)-receptor interaction, transforming growth factor (TGF)-beta signaling, Hippo signaling, among others (*Figure 1E*). To gain further insights into the functional implications of the identified genes, we employed the BottleNeck, Closeness, and EcCentricity algorithms to construct PPI networks for the top 20 genes (*Figure 1F-1H*) and the analysis revealed intricate connectivity patterns, shedding light on potential key players within the interactome.

Identification of seven genes as potential predictors of PA

We identified seven common genes (*SELL*, *ATF3*, *ITPR1*, *POMC*, *FASN*, *FOXO1*, and *CXCR4*) within the PPI networks using the BottleNeck, Closeness, and Eccentricity algorithms. Notably, these genes displayed reduced expression in PA samples from both GSE36314 and GSE119063 datasets, pointing to shared molecular mechanisms in PA onset and progression (*Figure 2A,2B*). To assess the diagnostic value of these genes, ROC curve analyses were conducted for each across the datasets. As shown in *Figure 2C,2D*, all seven genes showcased high AUC values, underlining their robust predictive capability for PA. Notably, related studies identified *ITPR1* as an autophagy-linked gene, positioning it as a central gene for our subsequent *in vitro* experiments.

Modulatory effects of ITPR1 overexpression and autophagy inhibition by 3-MA on PA progression

To study the role of *ITPR1* in HP75 and GH3 cell lines, we transfected these cells with an *ITPR1* overexpression plasmid (*Figure 3A,3B*). After successful transfection, we assessed the impact of *ITPR1* overexpression on autophagy-associated proteins Beclin1, LC3 I, and LC3 II, over different time intervals (12, 24, 48 hours). At 24 hours post-transfection, a marked induction of autophagy was evident, especially in the levels of LC3 I and LC3 II (*Figure 3C-3E*). Therefore, we selected the 24-hour interval for subsequent experiments. In the next phase, cells with overexpressed *ITPR1* were treated with the autophagy inhibitor Baf A1. This treatment resulted in elevated LC3 I and LC3 II protein levels. When combining *ITPR1* overexpression with Baf A1 treatment, we noticed even higher autophagy-related protein levels, suggesting a synergistic effect that amplifies autophagy (*Figure 3F-3H*). Our results pointed to a significant relationship between *ITPR1* overexpression and autophagy in PA cells, hinting at a potential pivotal mechanism in PA progression.

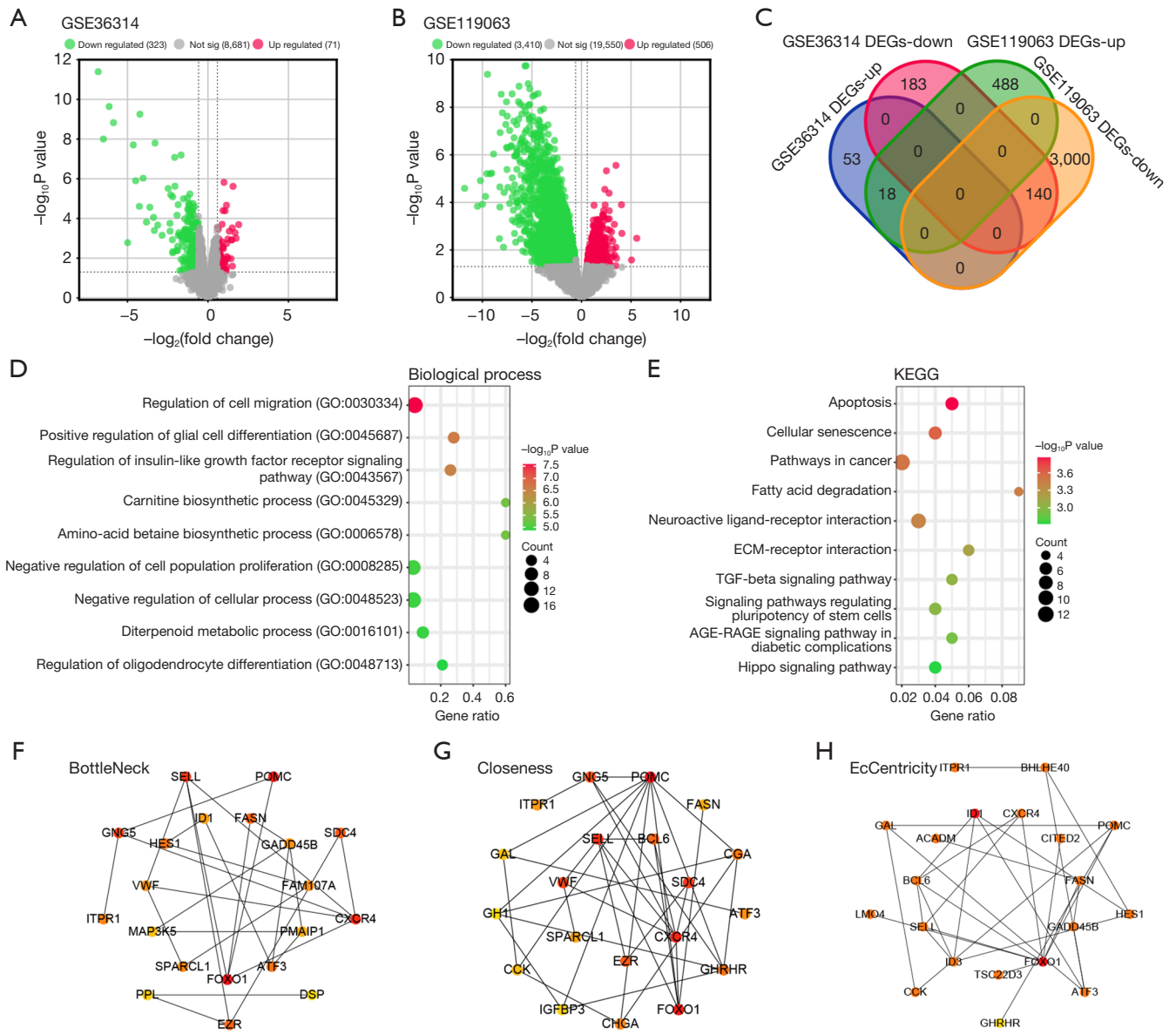

Figure 1 Screening and enrichment analysis of DEGs in GSE36314 and GSE119063. (A) The volcano map of DEGs in the GSE36314 dataset, the red scatter points indicate 71 up-regulated DEGs, and the green scatter points represent 323 down-regulated DEGs. (B) The volcano map of DEGs in the GSE119063 dataset, the red scatter points indicate 506 up-regulated DEGs, and the green scatter points represent 3,140 down-regulated DEGs. (C) The Venn diagram of DEGs in the two datasets, the green area on the left is 18 overlapping up-regulated DEGs, and the orange area on the right is 140 overlapping down-regulated DEGs. (D,E) Enrichment analysis was performed on 158 overlapping DEGs in BP and KEGG pathways. Bubble plots illustrating important GO terms and pathways identified in our study. The size of the circles correlates with the quantity of DEGs linked to each term, or pathway, and the color of the bubbles indicates the adjusted P value. (F-H) PPI networks of the top 20 genes, as identified by BottleNeck, Closeness, and EcCentricity algorithms, respectively. GO, Gene Ontology; KEGG, Kyoto Encyclopedia of Genes and Genomes; ECM, extracellular matrix; TGF, transforming growth factor; DEGs, differentially expressed genes; BP, biological process; PPI, protein-protein interaction.

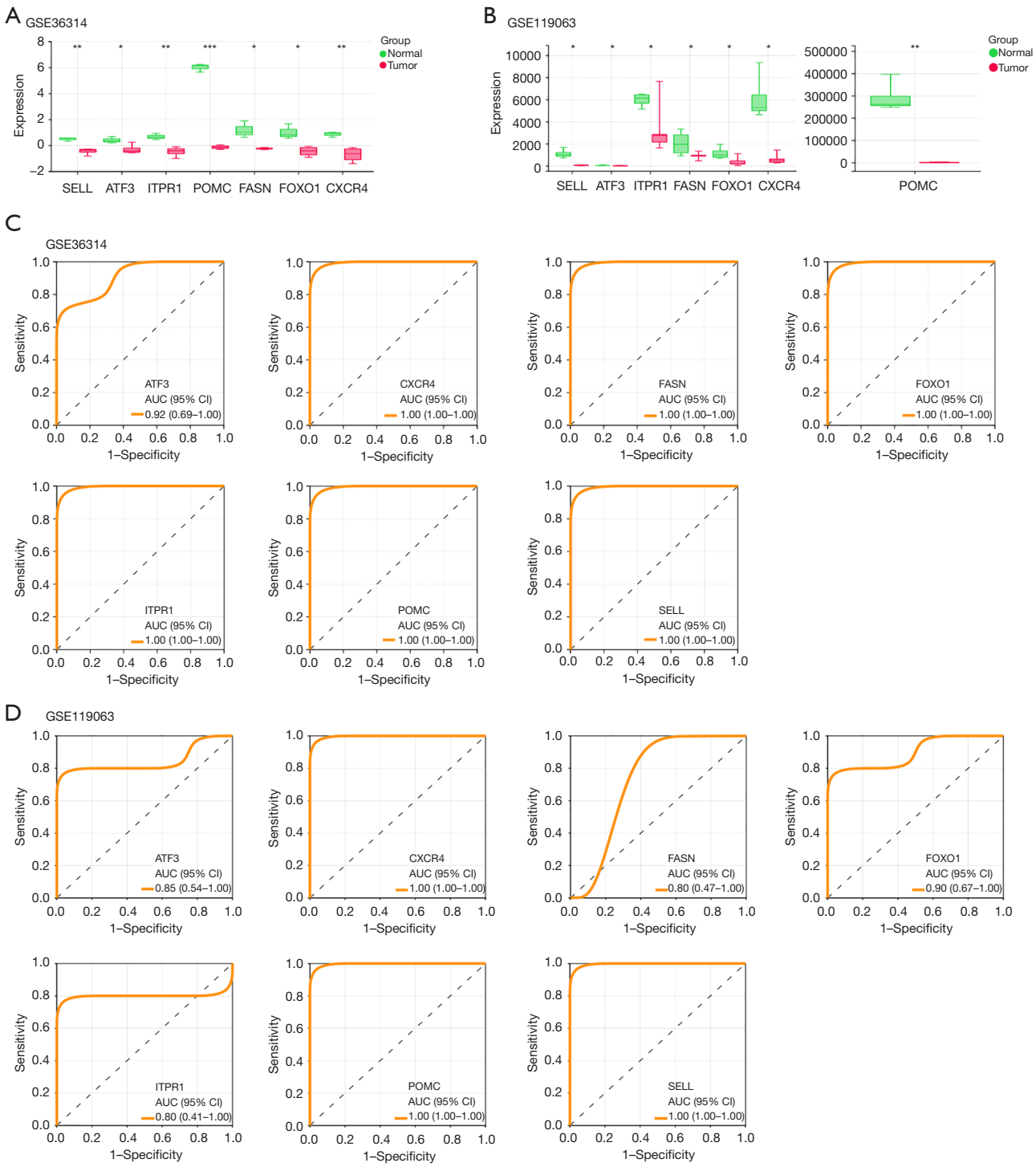

Figure 2 Assessment and ROC analysis of seven genes within the database. (A,B) The expression of seven genes in the GSE36314 and GSE119063 data sets, the red box line represents the tumor sample, and the green box line represents the normal sample. *, P<0.05; **, P<0.01; ***, P<0.001. (C,D) ROC curve analysis of seven key genes in the GSE36314 and GSE119063 datasets. The larger the AUC value, the higher the clinical diagnostic value. AUC, area under the curve; ROC, receiver operating characteristic.

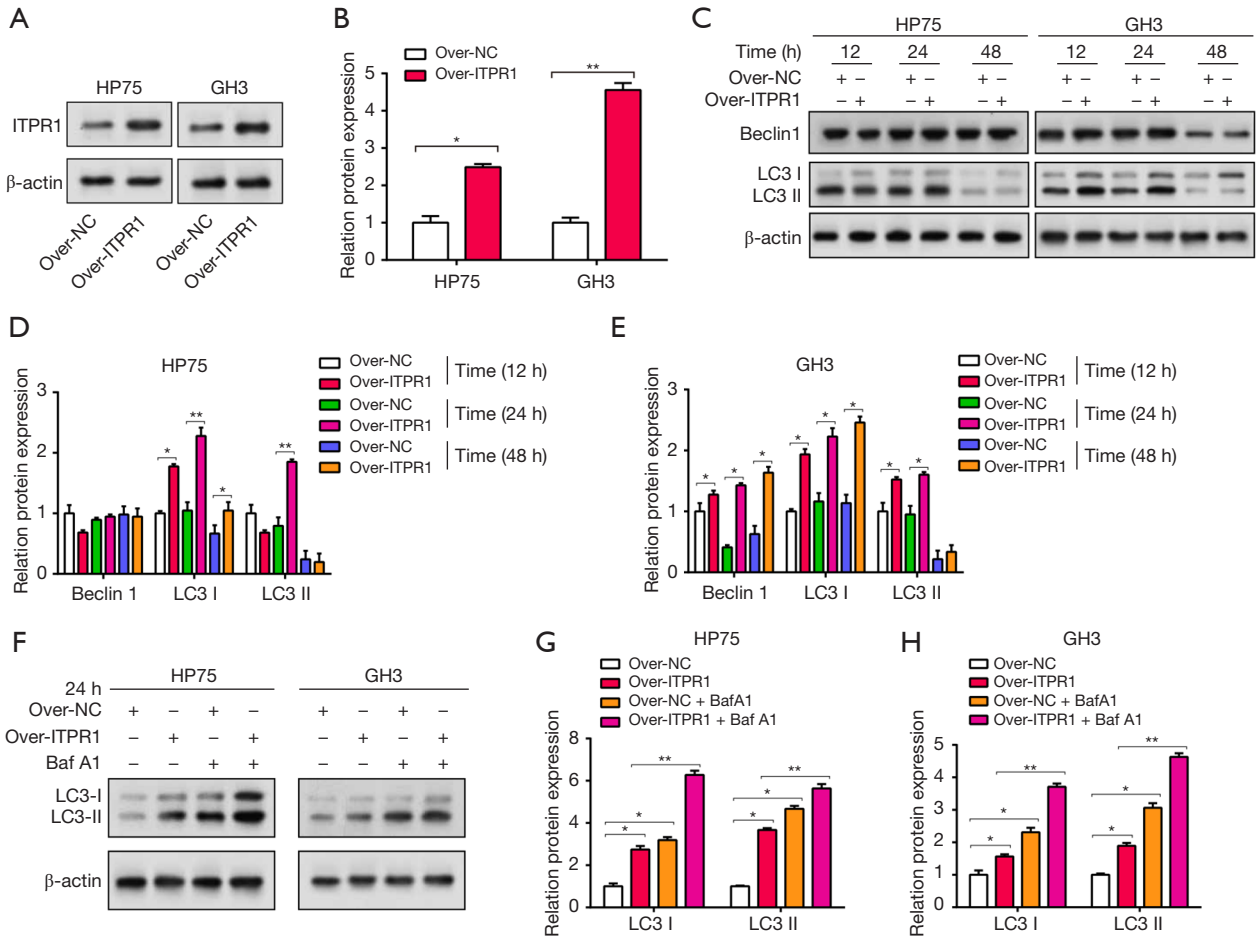

Figure 3 Overexpression of ITPR1 induces autophagy of vertical PAs. (A,B) The overexpression efficiency of ITPR1 in PA cells was detected by WB. (C-E) WB analysis of the expression of autophagy-related proteins Beclin1, LC3-I, and LC3-II in PA cells treated with overexpression of ITPR1 at different time periods (12, 24, and 48 hours). (F-H) WB analysis of the expression of autophagy-related proteins LC3-I and LC3-II in PA cells treated with overexpression of ITPR1 + autophagy inhibitor (Baf A1) for 24 hours. The bar graph on the right shows the results of the gray-scale detection of proteins. *, P<0.05; **, P<0.01. NC, negative control; PAs, pituitary adenomas; WB, western blotting.

Effect of ITPR1 on autophagy-mediated proliferation, movement, and infiltration of PA cells

In vitro experiments on HP75 and GH3 cells showed that *ITPR1* overexpression resulted in significant inhibition of cell proliferation, invasion, and migration, indicating the potential anti-tumor effects of *ITPR1*. In contrast, the autophagy inhibitor 3-MA was found to promote these cellular behaviors, suggesting that inhibition of autophagy may contribute towards PA progression. Interestingly, a relative attenuation of the competence of these cells was observed when overexpressed *ITPR1* was combined with 3-MA, suggesting a potential mitigating effect of *ITPR1* on the pro-tumor activity promoted by autophagy inhibition (*Figure 4A-4H*). Further WB analysis of the autophagy-related proteins LC3 I and LC3 II confirmed these findings. Overexpressed *ITPR1* caused an increase in these proteins in PA cells, indicating enhanced autophagy. In contrast, addition of 3-MA resulted in downregulation of these proteins. However, the combination of overexpressed *ITPR1* and 3-MA exhibited a regulatory effect that counteracted the inhibitory effect of 3-MA on apoptotic proteins (*Figure 4I-4K*). Collectively, these findings elucidate the complex interplay between *ITPR1*, autophagy, and tumorigenesis in PA cells, suggesting that manipulation of

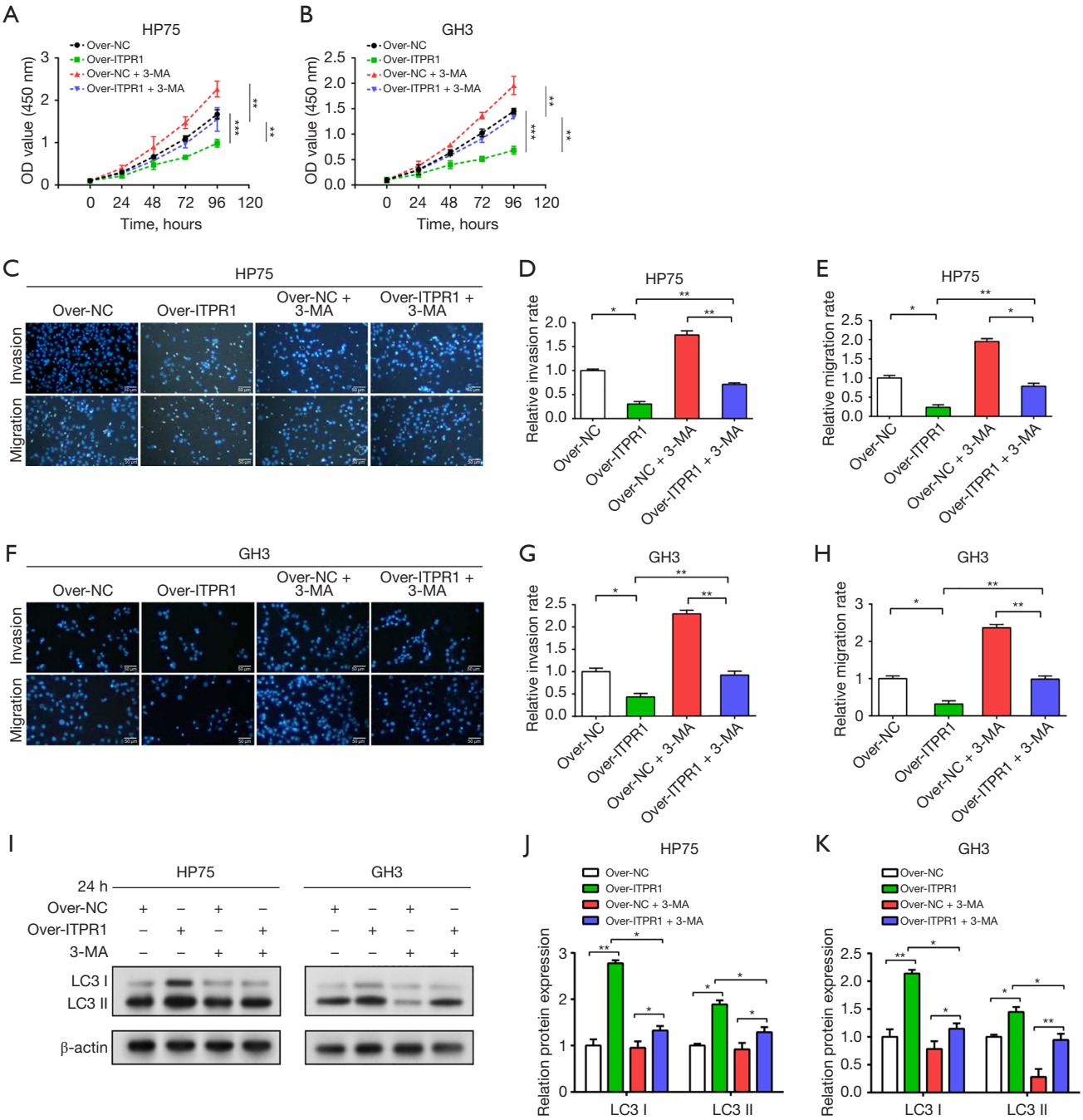

Figure 4 Effects of *ITPR1* overexpression and 3-MA co-treatment on proliferation, migration, invasion and autophagy of PA cells. (A,B) CCK-8 detected the regulation of *ITPR1* overexpression combined with 3-MA on cell proliferation in PAs cells. (C-H) Transwell analysis of the regulation of *ITPR1* overexpression combined with 3-MA on cell migration and invasion in PA cells. On the left is the business map under the microscope, and on the right is the quantified result (DAPI staining, scale 50 μm). (I-K) Western blotting analysis of the expression of autophagy-related proteins (LC3 I, LC3 II) after *ITPR1* overexpression combined with 3-MA in PA cells. The bar graph on the right shows the results of the gray-scale detection of proteins. *, P<0.05; **, P<0.01; ***, P<0.001. NC, negative control; OD, optical density; 3-MA, 3-Methyladenine; PAs, pituitary adenomas; CCK-8, cell counting kit-8; DAPI, 4',6-diamidino-2-phenylindole.

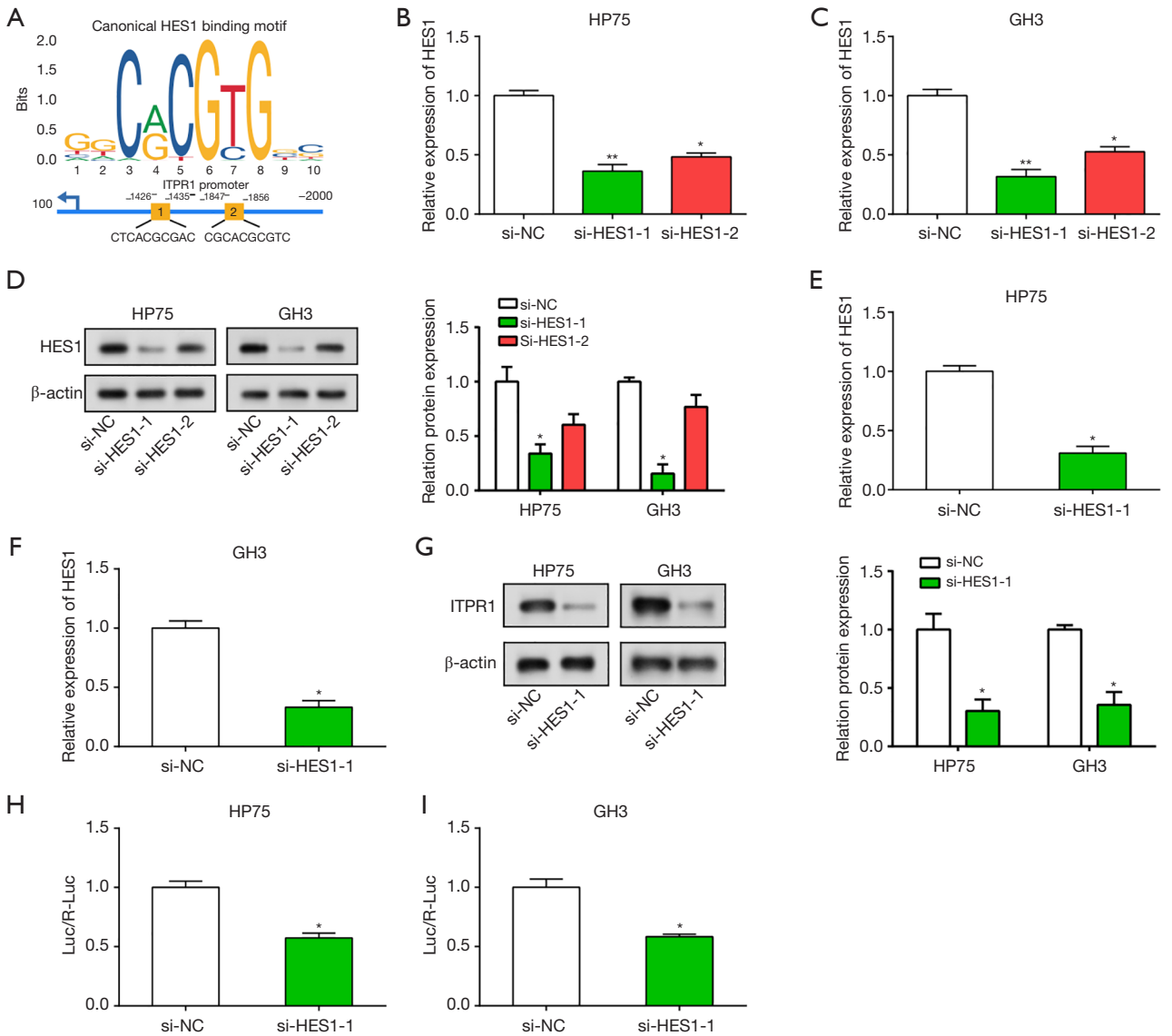

Figure 5 *HES1* acts as an upstream regulator of *ITPR1* in PAs cells. (A) The JASPAR database showed the binding site between *HES1* and *ITPR1*. (B-D) The knockdown efficiency of *HES1* in PA cells was detected by quantitative reverse transcription polymerase chain reaction and WB. The bar graph on the right side of the WB diagram shows the gray scale results of the protein detection. (E-G) The mRNA and protein expression levels of *ITPR1* in PA cells were detected by qRT-PCR and WB after *HES1* knockdown. The bar graph on the right side of the WB diagram shows the gray scale results of the protein detection. (H,I) Luciferase reporter assay assessed *ITPR1* promoter transcriptional activity upon *HES1* silencing. *, P<0.05; **, P<0.01. NC, negative control; PAs, pituitary adenomas; qRT-PCR, quantitative real-time polymerase chain reaction; WB, western blotting.

this tripartite relationship may provide potential therapeutic strategies for PA.

HES1 modulates ITPR1 through transcriptional activation

Utilizing the JASPAR database for bioinformatic analysis, we pinpointed two *HES1* responsive elements likely to bind the *ITPR1* promoter (*Figure 5A*). We then used qRT-PCR and WB assays to evaluate *HES1* transfection efficiency in PA cells. Notably, si-*HES1*-2 resulted in a pronounced decrease in *HES1* expression, indicating successful *HES1* knockdown (*Figure 5B-5D*). These results position *HES1*

as an upstream regulator of *ITPR1* in PA cells. Additionally, *HES1* knockdown corresponded with reduced *ITPR1* expression (*Figure 5E-5G*). The transcriptional activity of the *ITPR1* promoter was also diminished, as reflected by the dual luciferase assays (*Figure 5H,5I*). These findings unveil a sophisticated regulatory interplay between *HES1* and *ITPR1*, underscoring the potential of targeting *HES1* for improved PA management.

HES1 suppresses metastasis through ITPR1-induced autophagy in PA

After overexpressing *ITPR1*, we observed upregulation of the autophagy proteins LC3 I and LC3 II using WB, highlighting the function of *ITPR1* in autophagy regulation (*Figure 6A-6C*). Interestingly, *HES1* knockdown seemed to negate the *ITPR1* overexpression effect on these proteins. Through CCK-8 and Transwell assays, we determined that reduced *HES1* expression dampened the enhancing impact of *ITPR1* overexpression on PA cell proliferation, invasion, and migration (*Figure 6D-6K*). Collectively, our findings underscore a nuanced relationship among *HES1*, *ITPR1*, and autophagy in PA cell behavior, hinting at the potential of this regulatory triad as a therapeutic target in PA.

Discussion

PA comprise about 15–20% of intracranial tumors, establishing them as a prevalent subtype of intracranial neoplasms (23). The considerable heterogeneity observed in the clinical presentations and biological behaviors of PAs has spurred exhaustive research endeavors to elucidate their pathogenesis and pinpoint novel therapeutic targets (4). Among the many factors involved in the pathogenesis of PA, autophagy, a key cellular mechanism that helps maintain cellular homeostasis, has attracted considerable academic attention (24). Dysregulation of autophagy is linked to a variety of disorders. involving cancer (25). Emerging evidence suggests its potential involvement in the pathogenesis of PA (26). The utilization of bioinformatics has evolved as a formidable instrument for probing the complex molecular underpinnings of disorders such as PA (27). Analyzing high-throughput genetic data facilitates the identification of potential biomarkers and therapeutic targets, encompassing those pertinent to autophagy (28,29). Consequently, the amalgamation of bioinformatics with autophagy research augments the prospects for advancing our comprehension of PA pathobiology and pinpointing innovative therapeutic approaches.

From the GSE36314 and GSE119063 datasets, we analyzed a total of 158 overlapping DEGs. Bioinformatics analyses illuminated that these DEGs were notably enriched with BPs and pathways integral to the development and progression of PA and autophagy. Notably, the regulation of cell migration, pivotal for tumor invasion and metastasis, is extensively implicated in PA. Dysregulated cell migration could instigate aggressive tumor behaviors, potentially accounting for the observed clinical variability in PA outcomes. Intriguingly, these DEGs demonstrated significant enrichment in several pivotal pathways such as apoptosis, cellular senescence, fatty acid degradation, ECM-receptor interaction, TGF-β signaling, and Hippo signaling. For instance, both the apoptotic pathway and cellular senescence are recognized as fundamental tumor-suppressive mechanisms (30,31). Conversely, disruptions in these mechanisms could potentially foster tumorigenesis (32,33), which implies their potential involvement in PA. Similarly, the Hippo signaling pathway, a paramount regulator of organ size and tumor suppression, is implicated in the pathophysiology of autophagy (34). Together, these observations emphasize the prospective engagement of the identified DEGs in central BPs and pathways pertinent to PA pathogenesis and autophagy. These observations enhance our comprehension of the molecular underpinnings of PA and establish a strong groundwork for future investigations.

Our exploration spotlighted seven genes (*SELL*, *ATF3*, *ITPR1*, *POMC*, *FASN*, *FOXO1*, and *CXCR4*) as prospective biomarkers for PA, attributed to their notably reduced expression in PA samples from the GSE36314 and GSE119063 datasets. Importantly, *ITPR1*, recognized as an autophagy-associated gene, emerged as particularly significant. Gu *et al.* have evidenced its correlation with survival in breast cancer (35), further underscoring its clinical significance. The predictive accuracy of *ITPR1*, as well as the other genes, was substantiated by the AUC values derived from ROC curve analysis. Furthermore, the role of *ITPR1* in PA was more comprehensively elucidated using HP75 and GH3 cell lines. The overexpression of *ITPR1* coincided with heightened levels of autophagy-related proteins, namely Beclin1, LC3 I, and LC3 II, implying a pivotal role for *ITPR1* in instigating autophagy within PA. Notably, Beclin 1, a central figure in the initiation of autophagy, demonstrated upregulated expression, a common indicator of augmented autophagic activity. Similarly, LC3 I and LC3 II, crucial constituents in

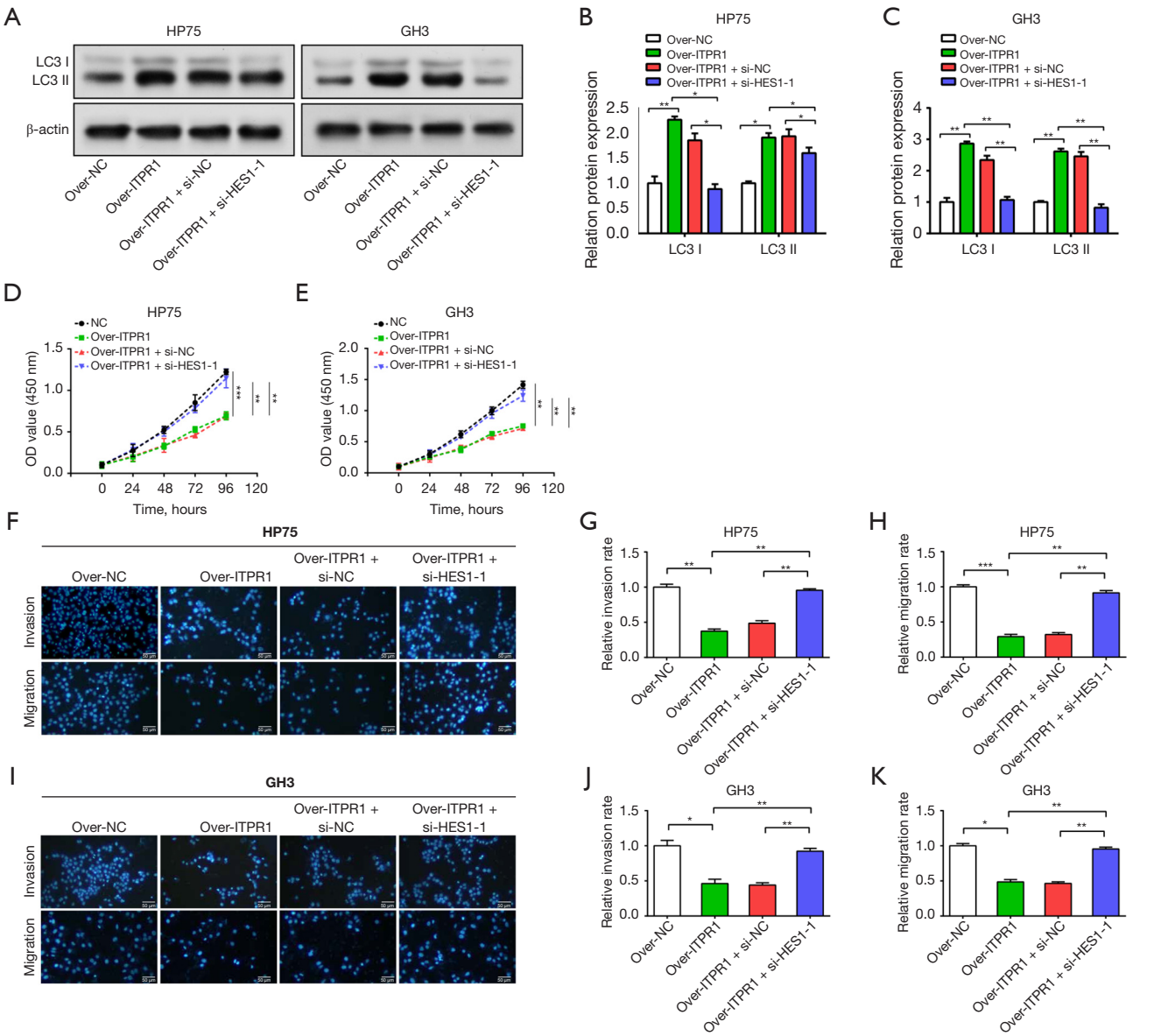

Figure 6 Impact of *HES1* knockdown and *ITPR1* overexpression on autophagy and tumorigenic behaviors in PAs cells. (A-C) The protein levels of apoptosis-related proteins (LC3 I, LC3 II) were detected by western blotting after knockdown of *HES1* and *ITPR1* overexpression in PA cells. The bar graph on the right shows the results of the gray-scale detection of proteins. (D-E) CCK-8 detected the effect of knockdown of *HES1* and overexpression of *ITPR1* in PA cells on cell proliferation. (F-K) Transwell detected the effect of knockdown of *HES1* and overexpression of *ITPR1* in PA cells on cell migration and invasion (DAPI staining, scale 50 μm). *, P<0.05; **, P<0.01; ***, P<0.001. NC, negative control; OD, optical density; PAs, pituitary adenomas; CCK-8, cell counting kit-8; DAPI, 4',6-diamidino-2-phenylindole.

autophagosome formation, displayed elevated levels, further affirming the association between *ITPR1* overexpression and autophagy induction. Additionally, we explored the use of the autophagy inhibitor Baf A1, an inhibitor of lysosomal ATPase that hinders the merging of autophagosomes and lysosomes (36). Upregulation of LC3 I and LC3 II protein levels after Baf A1 treatment, particularly in conjunction with *ITPR1* overexpression, suggests a synergistic effect that amplifies autophagy. This interaction underscores the critical role of *ITPR1* overexpression in autophagy

regulation and the progression of PA, deepening our insights into its molecular pathogenesis.

In our study on the intricate mechanisms driving PA development and progression, we investigated the effects of *ITPR1* overexpression and 3-MA, an autophagy inhibitor. Our results underscore an anti-tumorigenic role for *ITPR1*; its overexpression notably hindered PA cell behaviors linked to tumorigenesis. In contrast, 3-MA bolstered these pro-tumorigenic behaviors, pointing to the potential of autophagy modulation in PA therapy. Remarkably, combining *ITPR1* overexpression with 3-MA treatment led to a subdued cellular response, implying *ITPR1* might counterbalance the pro-tumorigenic outcomes of autophagy inhibition. This hypothesis gained traction in our WB analysis, where the joint application of *ITPR1* overexpression and 3-MA altered protein expression, reducing the suppressive effects of 3-MA on autophagy-associated proteins.

Extending these observations, we further elucidated the regulatory environment involving *HES1*, a potential upstream regulator of *ITPR1*. Using bioinformatics tools, we discovered two *HES1*-responsive elements within the *ITPR1* promoter region. These findings are consistent with study by Perrone *et al.*, which highlighted the critical role of the Notch system target gene *HES1* in the pathogenesis of PAs (37). They observed a positive correlation between *HES1* expression and NOTCH1, 2, 4 receptors, indicating activation of the Notch pathway in certain tumors. This suggested that targeting the Notch pathway, including *HES1*, has potential therapeutic advantages in the treatment of PAs. In our study, *HES1* knockdown, verified by qRT-PCR and WB assays, corresponded to a reduction in *ITPR1* expression, which provides support for the hypothesis of *HES1*-mediated transcriptional control of *ITPR1*. This theory was further supported by the dual luciferase assay results, in which *HES1* knockdown resulted in reduced *ITPR1* promoter activity. Our in-depth exploration of the functional role of *HES1* in regulating PA cell behavior and autophagy revealed that *HES1* knockdown counteracted the effects of *ITPR1* overexpression on autophagy proteins and also weakened the suppressive impact of *ITPR1* on PA cell growth, invasion and migration. These observations are consistent with the findings of Monahan *et al.* (38), who demonstrated that *HES1* is associated with PA cell proliferation and affects the expression of cell cycle inhibitors. Collectively, our results elucidate a complex regulatory interplay involving *HES1*, *ITPR1*, and autophagy in PA progression. These novel insights not only confirm existing research, while also laying the groundwork for the creation of innovative therapeutic approaches for PA.

Conclusions

In summary, our research elucidates the complex regulatory interactions between *HES1*, *ITPR1*, and autophagy in PA progression. We identified the pivotal role of *HES1* in modulating *ITPR1* expression, driving autophagy in PA cells, and subsequently curbing tumor invasiveness. These insights emphasize the therapeutic potential of targeting the *HES1-ITPR1*-autophagy pathway to counteract tumor advancement, presenting a new strategy for addressing treatment-resistant PA.

Acknowledgments

Funding: None.

Footnote

Reporting Checklist: The authors have completed the MDAR reporting checklist. Available at https://tcr.amegroups.com/article/view/10.21037/tcr-23-1320/rc

Data Sharing Statement: Available at https://tcr.amegroups.com/article/view/10.21037/tcr-23-1320/dss

Peer Review File: Available at https://tcr.amegroups.com/article/view/10.21037/tcr-23-1320/prf

Conflicts of Interest: All authors have completed the ICMJE uniform disclosure form (available at https://tcr.amegroups.com/article/view/10.21037/tcr-23-1320/coif). The authors have no conflicts of interest to declare.

Ethical Statement: The authors are accountable for all aspects of the work in ensuring that questions related to the accuracy or integrity of any part of the work are appropriately investigated and resolved. The study was conducted in accordance with the Declaration of Helsinki (as revised in 2013).

References

1. Liu X, Wang R, Li M, et al. Pituitary adenoma or pituitary neuroendocrine tumor: a narrative review of controversy and perspective. Transl Cancer Res 2021;10:1916-20.
2. Banskota S, Adamson DC. Pituitary Adenomas: From Diagnosis to Therapeutics. Biomedicines 2021;9:494.
3. Daly AF, Beckers A. The Epidemiology of Pituitary Adenomas. Endocrinol Metab Clin North Am 2020;49:347-55.
4. Melmed S, Kaiser UB, Lopes MB, et al. Clinical Biology of the Pituitary Adenoma. Endocr Rev 2022;43:1003-37.
5. Giuffrida G, D'Argenio V, Ferraù F, et al. Methylome Analysis in Nonfunctioning and GH-Secreting Pituitary Adenomas. Front Endocrinol (Lausanne) 2022;13:841118.
6. Aflorei ED, Korbonits M. Epidemiology and etiopathogenesis of pituitary adenomas. J Neurooncol 2014;117:379-94.
7. Mahzari M, Alhamlan KS, Alhussaini NA, et al. Epidemiological and clinical profiles of Saudi patients with hyperprolactinemia in a single tertiary care center. Ann Saudi Med 2022;42:334-42.
8. Bello MO, Garla VV. Gigantism and Acromegaly. Treasure Island, FL, USA: StatPearls Publishing, 2023.
9. Tritos NA, Miller KK. Diagnosis and Management of Pituitary Adenomas: A Review. JAMA 2023;329:1386-98.
10. Raverot G, Ilie MD, Lasolle H, et al. Aggressive pituitary tumours and pituitary carcinomas. Nat Rev Endocrinol 2021;17:671-84.
11. Arafah BM, Nasrallah MP. Pituitary tumors: pathophysiology, clinical manifestations and management. Endocr Relat Cancer 2001;8:287-305.
12. Lin AL, Donoghue MTA, Wardlaw SL, et al. Approach to the Treatment of a Patient with an Aggressive Pituitary Tumor. J Clin Endocrinol Metab 2020;105:3807-20.
13. Molitch ME. Diagnosis and Treatment of Pituitary Adenomas: A Review. JAMA 2017;317:516-24.
14. Rakesh R, PriyaDharshini LC, Sakthivel KM, et al. Role and regulation of autophagy in cancer. Biochim Biophys Acta Mol Basis Dis 2022;1868:166400.
15. Li C, Wei C, Zhao G, et al. Cancer cells remodeling and quality control are inextricably linked to autophagy. AIMS Molecular Science 2023;10:109-26.
16. Folkerts H, Hilgendorf S, Vellenga E, et al. The multifaceted role of autophagy in cancer and the microenvironment. Med Res Rev 2019;39:517-60.
17. Lyu L, Hu Y, Yin S, et al. Autophagy inhibition enhances anti-pituitary adenoma effect of tetrandrine. Phytother Res 2021;35:4007-21.
18. Kun Z, Yuling Y, Dongchun W, et al. HIF-1α Inhibition Sensitized Pituitary Adenoma Cells to Temozolomide by Regulating Presenilin 1 Expression and Autophagy. Technol Cancer Res Treat 2016;15:NP95-NP104.
19. Mangla A, Guerra MT, Nathanson MH. Type 3 inositol 1,4,5-trisphosphate receptor: A calcium channel for all seasons. Cell Calcium 2020;85:102132.
20. Raimondi L, Ciarapica R, De Salvo M, et al. Inhibition of Notch3 signalling induces rhabdomyosarcoma cell differentiation promoting p38 phosphorylation and p21(Cip1) expression and hampers tumour cell growth in vitro and in vivo. Cell Death Differ 2012;19:871-81.
21. Ochi S, Imaizumi Y, Shimojo H, et al. Oscillatory expression of Hes1 regulates cell proliferation and neuronal differentiation in the embryonic brain. Development 2020;147:dev182204.
22. Prakash V, R Patel S, Hariohm K, et al. Importance of squatting and sitting on the floor: perspectives and priorities of rural Indian patients with stroke. Top Stroke Rehabil 2016;23:240-4.
23. Pathak K, Pathak M, Patel N, et al. Classification of Brain Tumor Using Convolutional Neural Network. 2019 3rd International conference on Electronics, Communication and Aerospace Technology (ICECA). Coimbatore: IEEE, 2019:128-32.
24. Loos B, Klionsky DJ, Du Toit A, et al. On the relevance of precision autophagy flux control in vivo - Points of departure for clinical translation. Autophagy 2020;16:750-62.
25. Seranova E, Connolly KJ, Zatyka M, et al. Dysregulation of autophagy as a common mechanism in lysosomal storage diseases. Essays Biochem 2017;61:733-49.
26. Schepers J, Behl C. Lipid droplets and autophagy-links and regulations from yeast to humans. J Cell Biochem 2021;122:602-11.
27. Papathomas TG, Nosé V. New and Emerging Biomarkers in Endocrine Pathology. Adv Anat Pathol 2019;26:198-209.
28. Li N, Zhan X. Mitochondrial Dysfunction Pathway Networks and Mitochondrial Dynamics in the Pathogenesis of Pituitary Adenomas. Front Endocrinol (Lausanne) 2019;10:690.

29. Wang FH, Zhang XT, Li YF, et al. The Chinese Society of Clinical Oncology (CSCO): Clinical guidelines for the diagnosis and treatment of gastric cancer, 2021. Cancer Commun (Lond) 2021;41:747-95.
30. Di Micco R, Krizhanovsky V, Baker D, et al. Cellular senescence in ageing: from mechanisms to therapeutic opportunities. Nat Rev Mol Cell Biol 2021;22:75-95.
31. Delbridge AR, Valente LJ, Strasser A. The role of the apoptotic machinery in tumor suppression. Cold Spring Harb Perspect Biol 2012;4:a008789.
32. Puga A, Ma C, Marlowe JL. The aryl hydrocarbon receptor cross-talks with multiple signal transduction pathways. Biochem Pharmacol 2009;77:713-22.
33. Li F, Huangyang P, Burrows M, et al. FBP1 loss disrupts liver metabolism and promotes tumorigenesis through a hepatic stellate cell senescence secretome. Nat Cell Biol 2020;22:728-39.
34. Tang F, Christofori G. The cross-talk between the Hippo signaling pathway and autophagy:implications on physiology and cancer. Cell Cycle 2020;19:2563-72.
35. Gu Y, Li P, Peng F, et al. Autophagy-related prognostic signature for breast cancer. Molecular Carcinogenesis 2016;55:292-9.
36. Maharjan Y, Dutta RK, Son J, et al. Intracellular cholesterol transport inhibition Impairs autophagy flux by decreasing autophagosome-lysosome fusion. Cell Commun Signal 2022;20:189.
37. Perrone S, Zubeldia-Brenner L, Gazza E, et al. Notch system is differentially expressed and activated in pituitary adenomas of distinct histotype, tumor cell lines and normal pituitaries. Oncotarget 2017;8:57072-88.
38. Monahan P, Rybak S, Raetzman LT. The notch target gene HES1 regulates cell cycle inhibitor expression in the developing pituitary. Endocrinology 2009;150:4386-94.

Cite this article as: Qiu C, Yao Y, Hu S, Xu Y. *HES1* induces *ITPR1*-mediated autophagy to exert anti-metastatic effects in pituitary adenomas. Transl Cancer Res 2024;13(2):661-675. doi: 10.21037/tcr-23-1320

